Electrochemical Iron Recovery from Biologically Produced Magnetite via Iron Oxide/Hydroxide Conversion: First Steps towards Terrestrial and Martian Applications

Reza Fayaz[1,5,6], Fabio La Mantia[2,5,6], Michael Baune[1,6], Antoine Carissimo[3,5,6], Guillaume Pillot[3,5,6], Md Izzuddin Jundullah Hanafi[4,5], Thorsten M. Gesing[4,5], Sven Kerzenmacher[3,5,6]& Jorg Thöming[1,5,6]

[1]University of Bremen, Chemical Process Engineering Group (CVT), Leobener Strasse 6, 28359 Bremen, Germany
[2]University of Bremen, Energy Storage and Conversion Systems, Wiener Strasse 12, 28359 Bremen, Germany
[3]University of Bremen, Environmental Process Engineering Group (UVT), Leobener Strasse 6, 28359 Bremen, Germany
[4]University of Bremen, Institute of Inorganic Chemistry and Crystallography, Leobener Strasse 7, 28359 Bremen, Germany
[5]University of Bremen, MAPEX Center for Materials and Processes, Bibliothekstrasse 1, 28359 Bremen, Germany
[6]University of Bremen, Center for Environmental Research and Sustainable Technology (UFT), Leobener Strasse 6, 28359 Bremen, Germany

ABSTRACT

Ferrihydrite ($Fe_{10}O_{14}(OH)_2$), an iron oxide/hydroxide, is found in a variety of terrestrial and interplanetary environments. This study presents a novel combination of bio-leaching and electrolysis to address the need for efficient mining of low-grade iron resources. Iron-reducing bacteria biologically convert iron oxide/hydroxide to magnetite. This could then be magnetically extracted and electrolyzed at 363 K using an alkaline medium into metallic iron. The innovation could facilitate the exploitation of marginal iron reserves, particularly in areas where no rich ores are available. The process is also promising for adaptation to extraterrestrial sources such as Martian regolith.

In our research, *Carboxydothermus ferrireducens* converted superparamagnetic iron oxide/hydroxide (Fe(III)) into a ferrimagnetic (Fe(II)/Fe(III)) phase. After 20 hours of alkaline deoxidation electrolysis, this 'bio-magnetite' was electrochemically reduced to 25 wt.% of Fe(0). The iron yield was increased to 67 % by integrating a heat treatment step. This resulted in a high current efficiency of 63 % and an energy consumption of 17.9 MJ/kg, competitive with current industrial practices. The morphological and chemical changes induced by the heat treatment facilitated iron reduction and minimized parasitic hydrogen evolution. Improved reducibility of bio-mineralized materials was also observed. These findings suggest the potential of biotechnological approaches in metallurgy.

Keywords

Bio-mineralization, Electrometallurgy, Iron, Low-grade resources, Extraterrestrial Mining, In-situ resource utilization (ISRU)

Introduction

Iron is an important material worldwide and its demand is expected to increase[1]. As conventional iron smelting with coke leads to an enormous release of greenhouse gases combined with a very high energy turnover[2], the development of environmentally friendly alternatives is of crucial importance[3].

While the use of hydrogen in direct reduction processes is already a long tradition[4], deoxidation electrolysis has also been proposed and investigated to replace the current polluting production of iron[5,6,7]. However, efforts to date have mainly focused on high-value resources, while innovations that can utilize currently unusable iron resources could have significant economic and strategic impacts in the future.

Ferrihydrite, an iron oxide/hydroxide with variable iron content, is predominantly found as an amorphous phase in sands, sediments, and laterites[8]. It is also a major component of Fe-rich sludges derived from water treatment plants and mining and ore processing industries[9]. Due to its amorphous nature and association with various impurities, this iron oxide/hydroxide is not normally targeted for iron extraction. With high-grade iron ore reserves being depleted,

alternative approaches are being sought to convert low-grade ores into usable materials. Bio-remediation could offer a way to harness these currently under-exploited resources[10].

In addition, in-situ resource utilization (ISRU) of local resources for extraterrestrial oxygen and metal production is critical for future extended planetary exploration missions[11,12]. The local production of essential metals such as iron on Mars is emerging as a key factor for colonization and long-term sustainable habitation[13]. Under extraterrestrial conditions, resources are limited, so only raw materials such as Martian regolith and Martian brine can be used[14]. Regolith comprises several metal oxides, including Fe-bearing phases, in a complex mineralogy[15,16].

For converting regolith into metals using ISRU-generated electricity as the power source, electrolysis has been proposed[17]. However, current electrolytic methods produce uncontrollable metal composites. The state-of-the-art technology is molten regolith electrolysis (MRE) at high temperatures of 1873 K[18]. It only results in a partial reduction and the formation of a metallic mixture pool that requires further siphoning[19].

Another approach involves solid-state reduction, eliminating the need to melt the ore. The process uses a molten salt with a high potential window, solubility, and diffusivity for oxygen ions[20,21,22]. This solid-state approach does have the benefit of lower operating temperatures (around 1173 K) than MRE. However, a complete removal of oxygen and a selective extraction of the desired metals have not yet been achieved. Instead, these solid-state processes resulted in elemental microparticle inclusions embedded in much larger oxide grains, with the remaining oxide pellets containing dispersed spherical distributions of the product[23]. This inherent complexity of the resulting product after reduction would be a problem for practical applications.

This study introduces a novel energy-efficient concept for iron fabrication from low-grade resources by combining bio-leaching, magnetic extraction, and electrolysis. The bio-mineralization technique is known for forming magnetic minerals from sediments[10]. This also holds the potential for in-situ resource utilization but is still in the immature phase[24]. A series of biomining experiments performed on the International Space Station (ISS) showed no significant difference between gravity conditions, demonstrating the effectiveness of the process under different gravity regimes[25]. Concentrated ferrimagnetic iron oxide solutions were extracted from Martian and Lunar regolith using various microorganisms, but there was no further conversion to Fe(0)[26,27]. In addition, newer and mineralogically more accurate regolith simulants such as MGS-1[16] have not yet been tested. The feasibility of this novel concept remains to be thoroughly validated.

Metal oxides exhibit semiconducting properties that make direct electroreduction difficult due to their charge transfer resistance[28]. Nevertheless, we have shown that solid-state deoxidation electrolysis of iron oxides can be achieved even in an aqueous medium[5]. This paves the way for the electrowinning of iron from biologically produced magnetite via iron oxide/hydroxide conversion. During this alkaline electrolysis, oxygen ions are expelled from the pellets and diffuse to the inert anode to be discharged as oxygen gas.

Although bio-leaching has been employed for metal recovery from ores such as pyrite[29], the post-bio-leaching electrochemical behavior of under-exploited iron oxide/hydroxides such as ferrihydrite remains poorly understood. Our process uses naturally occurring iron-reducing bacteria to convert iron oxide/hydroxide into a magnetically responsive form. Based on the results of our previous study[5], we successfully used alkaline deoxidation electrolysis at 363 K to convert 25 wt.% of this bio-remediated Fe(II)/Fe(III) mineral to Fe(0). We also proposed an intermediate heat treatment step to increase the iron yield to 67 % with a reduced energy input. The process promises to make low-grade iron deposits economically viable and suggests a potential iron extraction strategy on Mars, where current methods are impractical.

Results and discussion

Ferrihydrite, an iron-rich component of various natural soils, industrial wastes, and Martian regolith, is classified as an iron oxide/hydroxide. In this study, we synthesized a chemically similar compound to serve as the starting material, selected for its ability to support microbial respiration under anoxic conditions. Due to the variable iron content and amorphous nature of ferrihydrite, we could not confidently confirm the identity of our synthesized material as ferrihydrite, referring to it instead as 'iron oxide/hydroxide'.

Bio-magnetite was produced by supplying this iron oxide/hydroxide to the iron-reducing bacterium *C. ferrireducens* as the terminal electron acceptor for anaerobic respiration. The concentration of Fe(II), measured spectrophotometrically after extraction in HCl, increased over time, reaching about 35 % of Fe(III) reduction after two days of cultivation (Figure 1a). A black magnetic material was formed and identified as magnetite using X-ray powder Bragg-Rietveld (XRPD) data (Supplementary S2). Microbial cells were observed at the surface of the particles (Figure 1b). These results align with what was previously reported for this iron-reducing species[30,31].

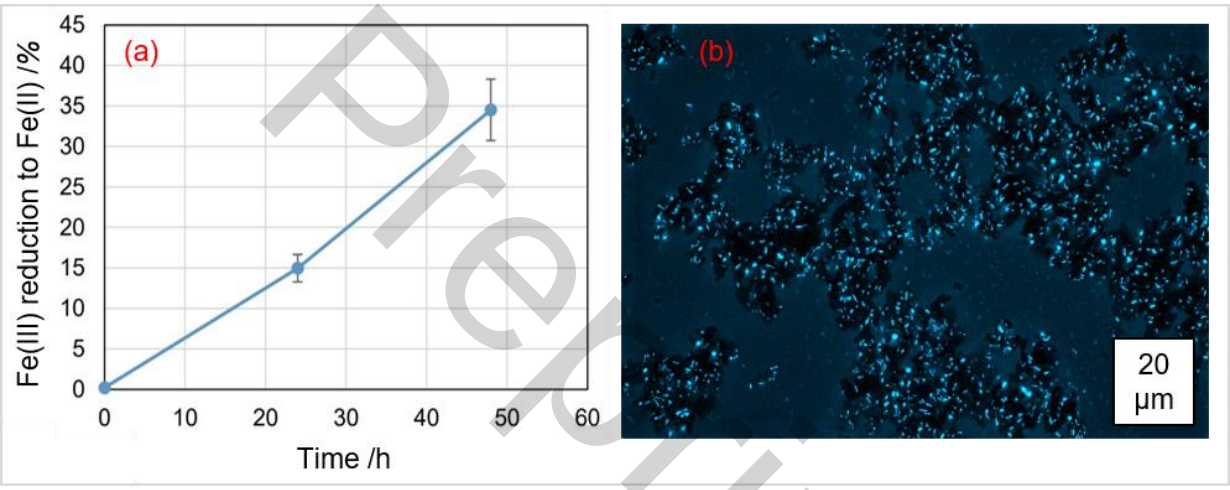

Figure 1. Growth of the iron-reducing bacterium with iron oxide/hydroxide. (a) The ratio of Fe(II) produced to the initial Fe(III) concentration, as a function of time. The average for three cultures is shown, with error bars indicating the standard deviation. (b) Black magnetic particles from *C. ferrireducens* cultures (2 days) were observed with fluorescent light, revealing the presence of microbial cells (blue) all over the particles.

The process diagram (Figure 2) illustrates the preparation of three different iron-based materials for alkaline electrolysis. It begins with iron oxide/hydroxide, which undergoes bio-mining to produce bio-magnetite. This bio-magnetite can either be used directly or further processed through heat treatment (1173 K, 3 h, under air) to examine the effects of chemical and microstructural alterations on electrochemical behavior. All three materials, iron oxide/hydroxide, bio-magnetite, and the heat-treated product, are then pelletized. These pellets serve as cathodes in an alkaline electrolysis setup operating with a 10 M NaOH solution at 363 K. Each pellet undergoes cathodic reduction at -1.4 V vs. Ag/AgCl for conversion to Fe(0). X-ray powder diffraction refinements (Supplementary S2) and Brunauer-Emmett-Teller (BET) analyses revealed changes in the crystal structure induced by bio-mining and heat treatment. Bio-mining reduced the specific surface area (SSA) from 285 m^2/g for the iron oxide/hydroxide to 41.5 m^2/g for bio-magnetite. XRPD data also confirm that bio-mining successfully converted a quantum-crystalline iron oxide/hydroxide with an average crystallite size (ACS) of 2.7(1) nm into a micro-crystalline bio-magnetite with an ACS of 16.2(2) nm (Table 1). Due to its high diffuse scattering content, the ACS of iron oxide/hydroxide could only be determined using the PDF EnvACS method[32] (Supplementary S3). This transformation can be explained by bacterial

metabolic activities so that the bacterial structures such as cell walls, membranes, or debris act as nucleation points for crystallization[33,34].
XRPD also confirmed the full oxidation of bio-magnetite (Fe(II)/Fe(III)) to a single (Fe(III)) phase ('bio-hematite') via heat treatment. Following this, the SSA further declined to 0.27 m²/g for bio-hematite, accompanied by an increase in the degree of crystallinity (DC) to 96(5) % and the ACS to 238(6) nm). The numbers in brackets represent the estimated standard deviations of the obtained values in the last digit.

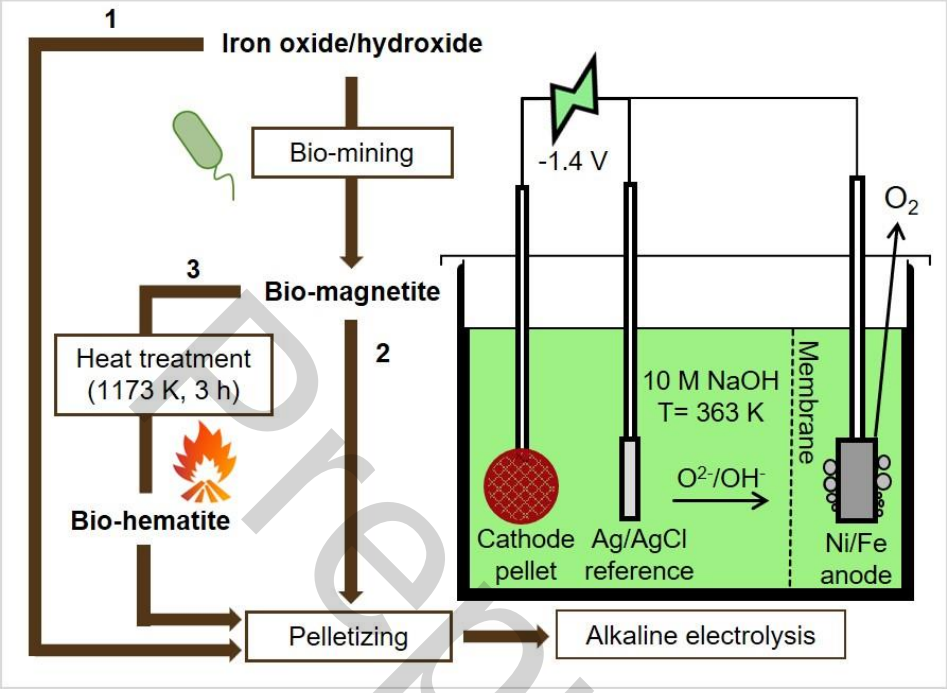

Figure 2. Schematic diagram showing the production process of bio-magnetite from iron oxide/hydroxide, followed by pelletizing with optional heat treatment. The pellets are then used in alkaline electrolysis for electrochemical conversion to Fe(0) at 363 K. Electrolysis is conducted in a two-compartment cell separated by an anion exchange membrane. The cathode pellets are then subjected to characterization analyses.

Table 1. The degree of crystallinity (DC), average crystallite size (ACS), and specific surface area (SSA) of the various feedstocks. The numbers in brackets are the estimated standard deviations of the obtained values in the last digit. (*) XRPD data of iron oxide/hydroxide shows broad humps associated with the quantum-crystalline phase which makes it impossible to distinguish the amorphous content.

Sample	DC /wt.%	ACS /nm	SSA /(m^2/g)
Iron oxide/hydroxide	*	2.7(1)	285
Bio-magnetite	80(5)	16.2(2)	41.5
Commercial magnetite	87(5)	74(1)	8.1
Bio-hematite	96(5)	238(6)	0.27
Commercial hematite	95(5)	135(1)	2.6
Heat-treated commercial hematite	99(5)	173(2)	0.76

A Comparative Electrochemical Analysis

To observe the changes caused by bio-mining and heat treatment on the electrochemical process of iron reduction, cyclic voltammetry (CV) and chronoamperometry tests were conducted for the starting iron oxide/hydroxide, bio-magnetite, and bio-hematite.

In the first CV cycles, the plots for the three materials tested are superimposed, with no discernible redox peaks (Supplementary S4), indicating that the iron oxide surfaces had not yet reached electrochemical activity. This initial lack of activity is consistent with the need for surface conditioning, where repeated cycling activates the material and enhances electron transfer. However, clear electrochemical behavior is apparent by the third CV cycle (Figure 3a). The cathodic current peak at approximately -1.3 V vs. Ag/AgCl reference electrode is attributed to iron reduction. For iron oxide/hydroxide and bio-magnetite, the reduction peaks start earlier than bio-hematite and show higher corresponding cathodic currents. The parasitic hydrogen evolution reaction (HER) starts in all samples shortly after the reduction peak of Fe(0) formation. However, the onset of the HER shows higher cathodic currents in bio-magnetite and the highest currents for iron oxide/hydroxide.

In addition, whereas there is a more pronounced boundary between the iron and HER peaks for bio-hematite, these appear to be more disruptive for iron oxide/hydroxide and bio-magnetite. During the anodic sweep, the corresponding anodic currents are higher for bio-magnetite, possibly due to high capacitive currents[35] or more likely due to superimposed Faradaic currents such as re-oxidation of hydrogen potentially trapped in the microstructure.

Consequently, electrolysis tests were conducted by applying a potential of -1.4 V vs. Ag/AgCl for 20 h. It should be noted that the application of a potential of -1.3 V vs. Ag/AgCl did not result in any reduction of iron cations. Likely, overcompensation of the mass transfer resistance caused by limiting diffusion in the boundary layers is required. The corresponding electrolysis currents were measured over time (Figure 3b) and the iron extraction yields were determined via XRPD.

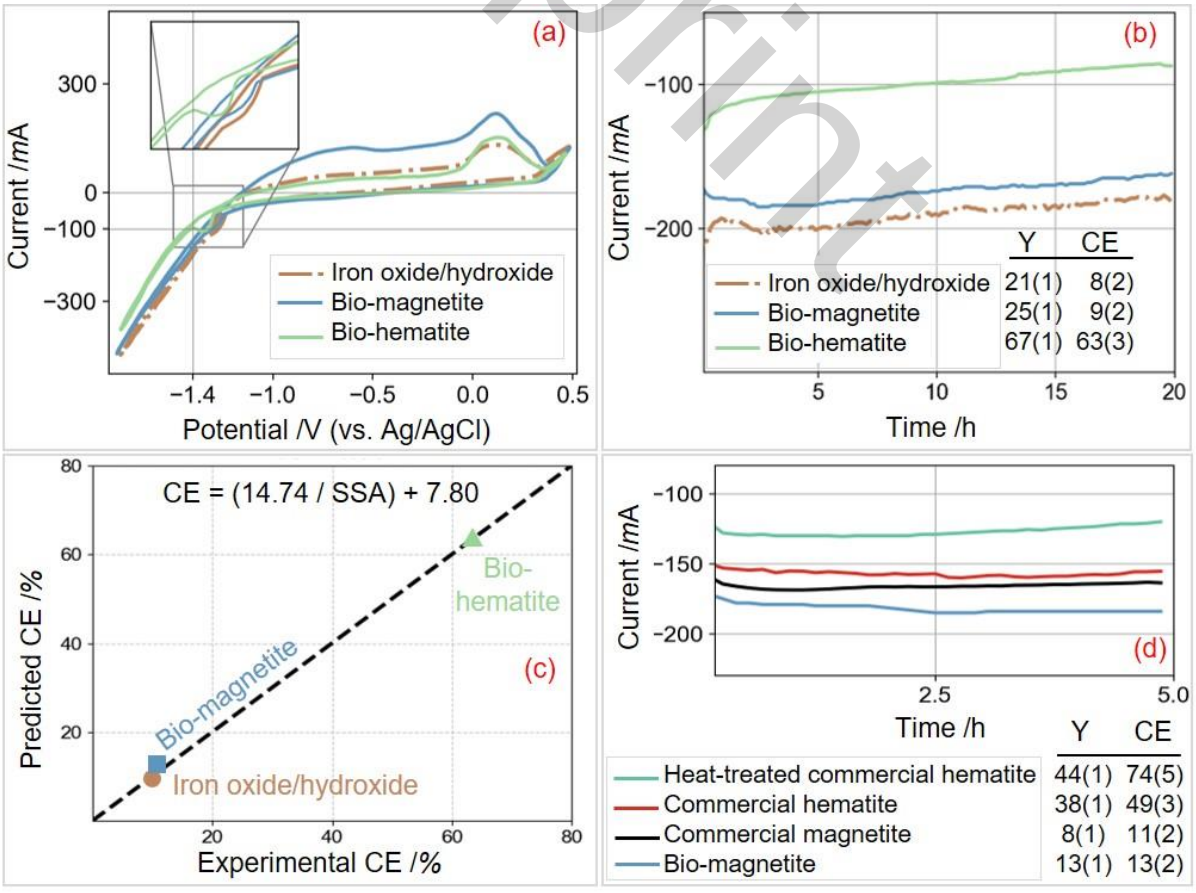

Figure 3. (a) The third cycle of cyclic voltammetry test and (b) the 20 h chronoamperometry result at -1.4 V vs. Ag/AgCl in 10 M NaOH for iron oxide/hydroxide as starting material, the biologically produced magnetite (bio-magnetite) and after heat treatment (bio-hematite) at 363 K and the obtained iron yields (Y) and current efficiencies (CE). (c) The parity plot presents a model for predicting the inverse correlation of current efficiency with specific surface area (SSA). (d) The comparison of reducibility of commercial hematite vs. that after heat treatment, and commercial magnetite vs. bio-magnetite by 5 h electrolysis is shown as iron yield Y/wt.% and current efficiency CE/%. The numbers in brackets are the estimated standard deviations of the obtained values in the last digit. Note that the results of the 20 h tests (b) and the 5 h tests (d) are not directly comparable due to the different test durations. The former focuses on the main materials, while the latter are control tests on additional materials.

The bio-hematite currents remain relatively low and with minimal fluctuations throughout the electrolysis, with an extracted iron yield of 67(1) wt.%. This stability is indicative of a more steady and efficient iron electrochemical reduction process. In contrast, iron oxide/hydroxide (yield: 21(1) wt.%) and bio-magnetite (yield: 25(1) wt.%) exhibit higher currents and fluctuations despite lower yields, suggesting a lower selectivity and a less desired reduction process. These observations can be attributed to thermodynamical and microstructural factors. Thermodynamically, the standard Gibs free energy, required for the further electrochemical decomposition to elemental iron, reduces from 1013.7 kJ/mol for (Fe(II)/Fe(III)) oxides to 749.3 kJ/mol for Fe(III) oxides [36].

Furthermore, with its higher average crystallite size, bio-hematite provides a crystal structure with reduced micro-strain and bulk point defects that ensure pathways for electron movement that are more defined and less disrupted, which increases the favorable iron reaction kinetics. While the surface defects and morphology of iron oxide/hydroxide and bio-magnetite act as active sites for unwanted HER side reactions or inconsistent electron transfer. The higher SSA and the smaller ACS of iron oxide/hydroxide and bio-magnetite also mean a higher surface-to-bulk volume, which increases the overall undesired electrochemical activity at the surface. Additionally, the hard and dense magnetite shell causes lower diffusivity[37], supporting the formation of dense iron layers around the particle during the reduction, prohibiting further iron reduction as it was also shown for the reduction of iron oxides with hydrogen[38].

An inverse relationship between the current efficiency (CE) and SSA for all three minerals is observable as shown in Supplementary (S5). The parity plot (Figure 3c) presents a model for predicting this correlation ($CE = 14.74 / SSA + 7.80$). The lower surface-to-bulk volume of bio-hematite means fewer active sites for parasitic HER and a more controlled contribution of electrons for iron reduction, with a high current efficiency of 63(3) %. In contrast, a higher surface area means more undesired electrochemical reactions as the efficiency decreases to 8(2) % for iron oxide/hydroxide and 9(2) % for bio-magnetite.

Zhang et al.[39] showed that nanostructured iron oxides as electrode material present challenges such as low thermodynamic stability and susceptibility to surface side reactions. Pervez et al.[40] additionally showed that the crystalline phases of iron oxide nanotubes demonstrated superior electrochemical performance compared to their amorphous counterparts. This enhanced behavior was attributed to the better crystallized part of a phase to provide a more defined path for ion diffusion and electron transport, as evidenced by our results.

From a microstructural perspective, one might have anticipated that iron oxide/hydroxide would be much less efficient than bio-magnetite due to its SSA being about seven times higher. However, thermodynamics seems to balance the scales, allowing more electrons to be dedicated to iron reduction despite the abundance of active sites and side reactions. This is why iron oxide/hydroxide achieves an iron yield and faradaic efficiency comparable to that of bio-magnetite.

The conversion of bio-hematite outperforms the other two materials in terms of iron yield, current efficiency, voltage efficiency, and energy consumption (Figure 4). The lower efficiency of the non-heat-treated samples suggests that more of the electrical energy is being diverted to non-productive processes. While bio-mining can act as an important upstream step in the extraction of iron oxide/hydroxides such as ferrihydrite from low-grade ore resources, intermediate oxidation using heat treatment is required to improve the further electrochemical behavior.

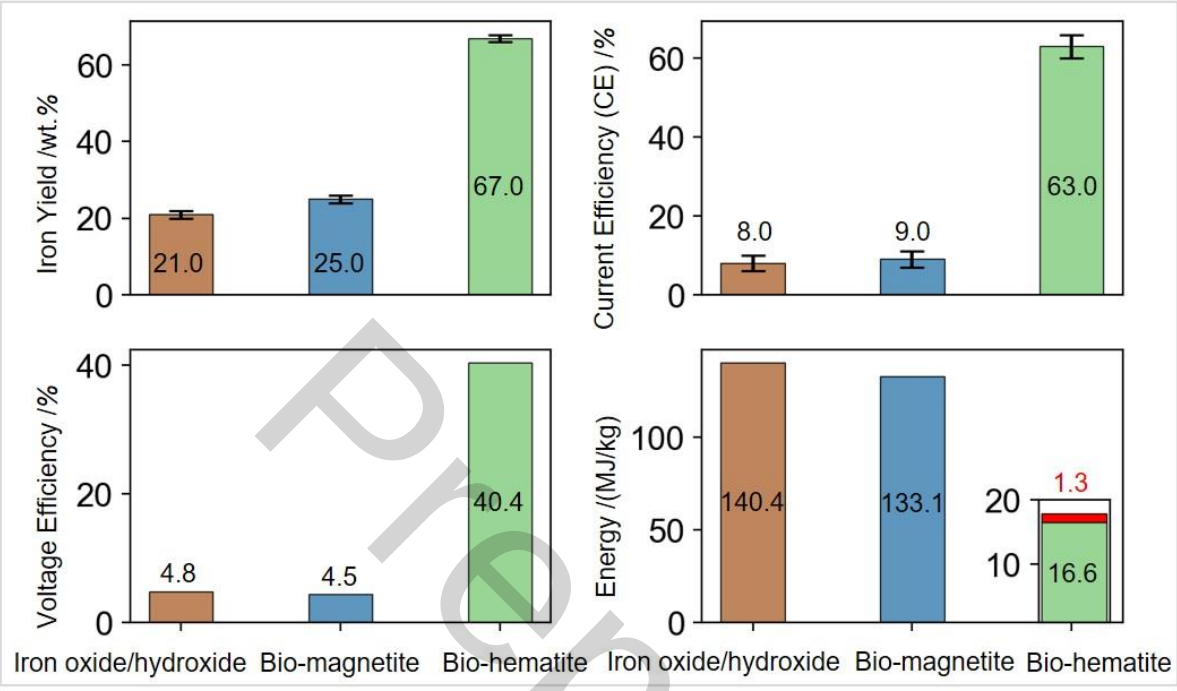

Figure 4. The values for iron extraction yield, current efficiency (CE), voltage efficiency, and energy consumption for iron oxide/hydroxide as the starting material, the biologically produced magnetite (bio-magnetite), and that after heat treatment (bio-hematite) after 20 h electrolysis at -1.4 V vs. Ag/AgCl in 10 M NaOH at 363 K. The error bars indicate the standard deviation. For bio-hematite, the required energy is divided into the energy for electrolysis (16.6 MJ/kg) and the additional energy for heating to 900 °C for heat treatment (1.3 MJ/kg).

In addition, bio-hematite requires a lower total cell voltage to maintain the applied cathodic potential, resulting in lower electrolysis energy consumption and better voltage efficiency. Even considering the required energy capacity for heating up to 900 °C for thermal treatment, the total energy consumption of bio-hematite is far lower than that of iron oxide/hydroxide and bio-magnetite. For calculating this electrolysis energy consumption, the average cell voltage was multiplied by the electrical charge per mass of iron produced. The result is 17.9 MJ/kg, which is also lower than the estimated energy consumption of 19 MJ/kg for an industrial blast furnace[41].

The SEM images of the highly amorphous and scattered iron oxide/hydroxide vs. the smoother and more uniform surface with agglomerated particles of bio-magnetite confirm the microstructural changes caused by the bio-leaching process as the cellular components act as the nucleation points for crystallization (Figure 5). A further decrease in surface defects and an increased agglomeration was achieved by the heat treatment process as it reduced surface irregularity and increased particle cohesion. In addition, the SEM image of a reduced bio-hematite after 20 hours of alkaline electrolysis shows areas where iron is inclusively present as individual phases. The elemental map data of the produced Fe(0) is represented in

Supplementary (S6).

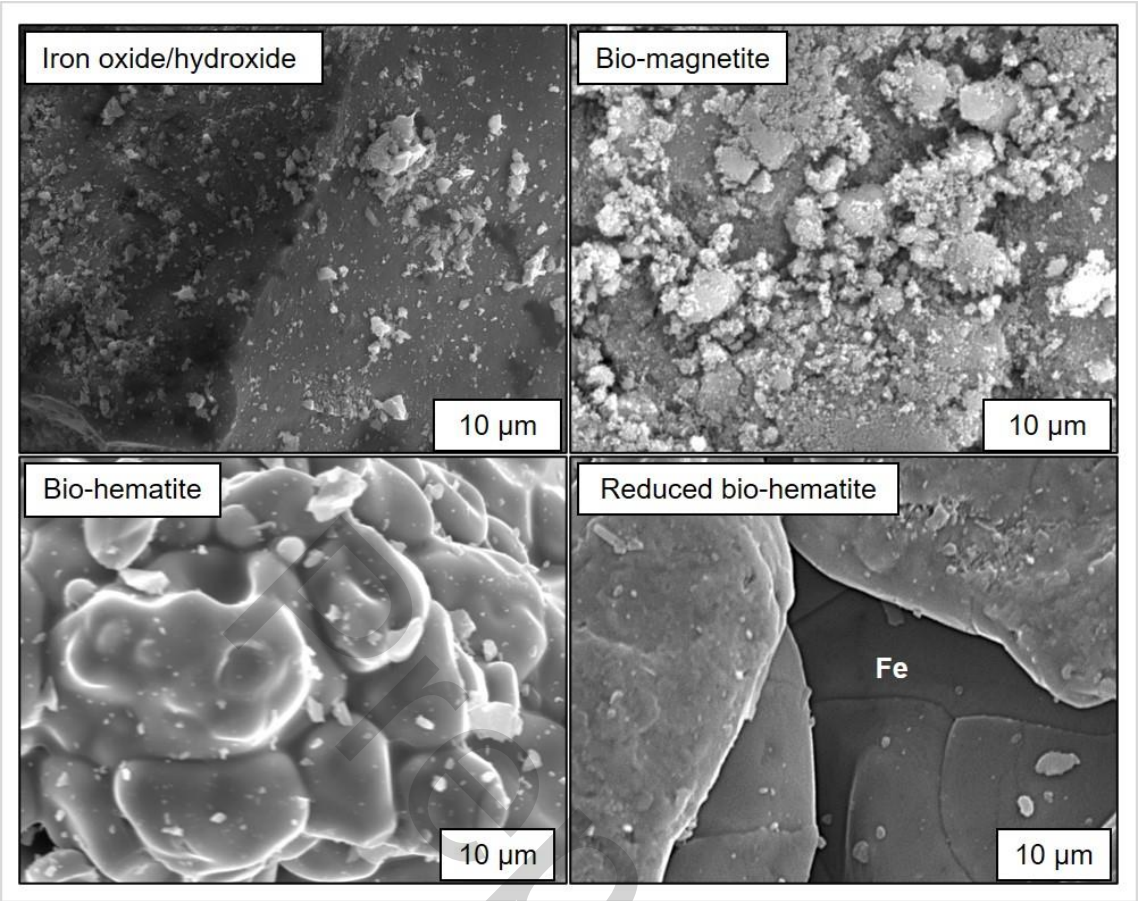

Figure 5. SEM images of iron oxide/hydroxide as the starting material, the biologically produced magnetite (bio-magnetite), and that after heat treatment (bio-hematite) confirm the microstructural changes during the bio-leaching and heat treatment processes. The image of a reduced bio-hematite after 20 h of electrolysis at -1.4 V vs. Ag/AgCl in 10 M NaOH at 363 K shows areas where Fe is inclusively present.

Mineral Transformation by Heat Treatment and Bio-leaching

To cross-check heat treatment effects on microstructure and reducibility, a set of control tests were conducted. Commercial hematite, with and without heat treatment, was subjected to alkaline electrolysis for 5 h. Commercial and biologically produced magnetite were also compared to gain a better insight into the impacts of bio-leaching. All electrolysis plots as well as the corresponding iron extraction yield and Faradaic efficiency are presented in Figure 3d. Note that these results are not directly comparable to the 20 h test results due to the different materials and test durations.

First, it can be seen that the reducibility of commercial hematite (both heat treated and untreated), with its single Fe(III) valence, outperforms commercial magnetite and bio-magnetite, as thermodynamically expected. The relatively less negative Gibbs free energy for these Fe(III) oxides suggests that under the same electrochemical conditions, they can be reduced to metallic iron more readily.

A comparative analysis of the microstructural properties of non-heat-treated commercial hematite (SSA: 2.6 m^2/g, DC: 95(5) %, ACS: 135(1) nm) and that after heat treatment (SSA: 0.76 m^2/g, DC: 99(5) %, ACS: 173(2) nm) confirms that thermal treatment results in a lower specific surface area and higher ACS (Table 1). Electrochemically, the heat treatment of commercial hematite led to a decline in the corresponding currents and in turn a higher iron

yield and current efficiency. This is further evidence of the influence of crystallinity and grain size on reducibility and side reactions. These observations, in line with the improvements noted in the previous section, corroborate the benefits of heat treatment in optimizing the electrochemical properties of iron oxides/hydroxides.

We also observed a superior reducibility of bio-magnetite compared to a commercial magnetite. We compared commercial magnetite, with SSA of 8.1 m^2/g, DC of 87(5) %, and ACS of 74(1) nm, to bio-magnetite synthesized from the iron oxide/hydroxide in this research, with SSA of 41.5 m^2/g, a DC of 80(5) %, and ACS of 16.2(2) nm. Theoretically, the microstructural properties of commercial magnetite might be expected to confer advantages due to its lower SSA, suggesting fewer active sites and potentially reduced parasitic reactions. Despite this, our results indicated that bio-magnetite demonstrated enhanced electrochemical behavior in terms of iron yield and current efficiency. This outcome may be influenced by the potential incorporation of cellular components within the bio-magnetite granules, leading to organic inclusions that could alter the morphological structure of the mineral[42].

EDX analysis revealed traces of carbon in the bio-magnetite sample (Supplementary S7), probably from decomposed microorganisms or the partial formation of siderite ($FeCO_3$). It is hypothesized that these organic residues could serve as binding sites to facilitate electron transfer, particularly enhancing iron reduction. The possible presence of siderite embedded within the bio-magnetite matrix could thermodynamically favor the reduction process. Previous studies suggest that the composition of the cultivation medium and specific parameters can influence mineral formation during bio-leaching, with siderite formation being reported in bicarbonate-buffered mediums like the one used in this research[43,44]. In particular, thermophilic iron-reducing microorganisms are known to produce mixtures of magnetite and siderite during the reduction of ferrihydrite[45,46]. Given the complexity of the bio-mineralization process, further studies are needed to confirm these findings fully.

Perspective

This research enabled us to identify a future approach for iron fabrication from low-grade iron resources such as the Martian regolith. The MGS-1 basaltic Mars regolith simulant is manufactured from a mixture of several rocks[16]. The composition consists of amorphous and crystalline phases. The composition list includes five iron-including minerals, namely olivine, hematite, magnetite, ferrihydrite, and Fe-carbonate, as well as their iron contents (Table 2). It is evidence that ferrihydrite, the investigated mineral in this study, is the major iron-bearing phase of Martian regolith.

Our attempt to reduce regolith directly using the alkaline electrolysis at 363 K did not lead to any metal production as aqueous solutions do not provide a high enough potential window to decompose the complicated mixed mineral phases of regolith. The current high-temperature methods of molten regolith (1873 K) and molten salt (1173 K) electrolysis are also not yet promising or practical. To enable iron recovery using alkaline electrolysis at moderate temperatures, it is necessary to first precipitate the ferrous phases.

We, therefore, see the perspective that with an optimized upstream bio-mining beneficiation step, the iron-containing phases could be converted to magnetically responsive forms. This property is crucial for isolating iron from regolith's complex mixture of minerals. An intermediate heat treatment step before electrochemical reduction will also be suggested based on the results of this study. The proposed concept for the fabrication of iron from Martian regolith is represented in Figure 6. Using Ni/Fe as a non-contaminating inert anode material also aligns with the trace presence of nickel in Martian meteorites.[47] We underscore the importance of ongoing research to validate the concept for the MGS-1 Martian regolith simulant.

Table 2. The mineral composition (manufacturer fact sheet) of MGS-1 Martian regolith simulant and the iron content of the iron-bearing phases.

Mineral	Total /wt.%	Iron /wt.%
Crystalline		
Plagioclase	27.1	-
Pyroxene	20.3	-
Olivine	13.7	29.3
Hematite	0.5	5.1
Magnetite	1.9	20.3
Amorphous		
Anhydrite	1.7	-
Basaltic Glass	22.9	-
Hydrated Silica	3.0	-
Mg-sulfate	4.0	-
Ferrihydrite	3.5	35.4
Fe-carbonate	1.4	9.9

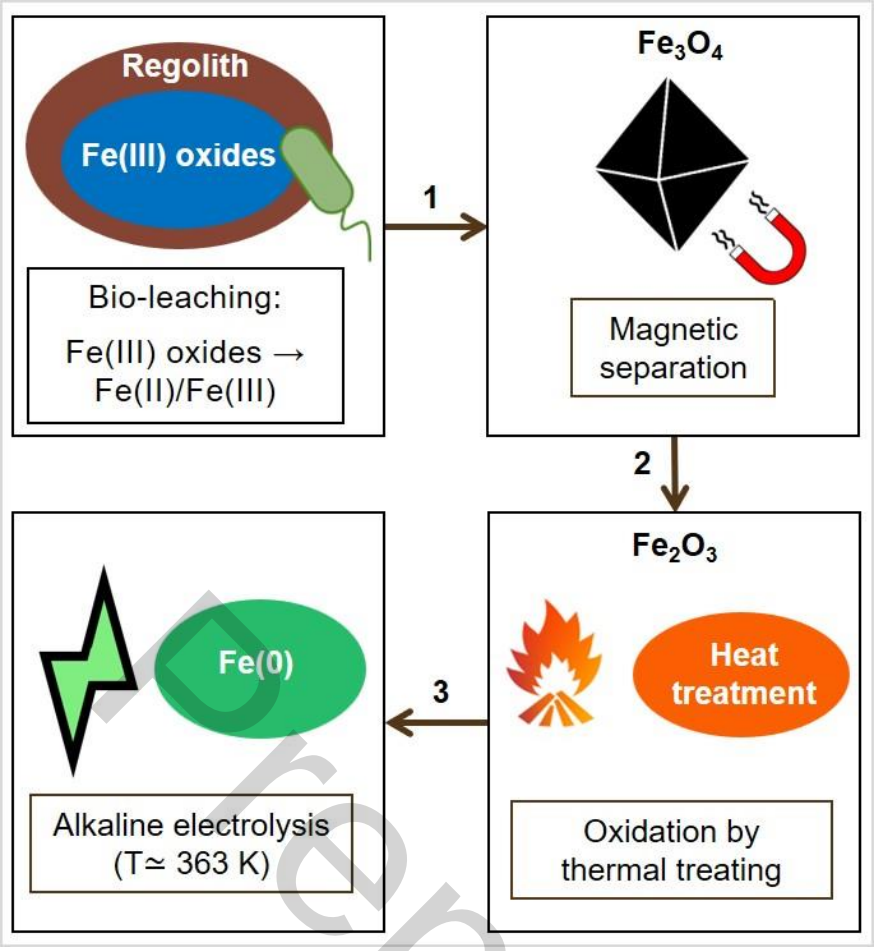

Figure 6. The proposed concept of alkaline deoxidation electrolysis with upstream bio-mining beneficiation and heat treatment for extraterrestrial iron fabrication from Martian regolith.

Furthermore, further investigations are required to modify the proportion of microbial cells present in the bio-mined minerals as we showed that this may possibly influence the electrochemical behavior. Depending on the microbial species and the cultivation conditions, iron-reducing microorganisms may rely on different extracellular electron transfer mechanisms and strategies to reduce iron oxides, including direct contact with the iron particles or electron shuttles (endogenous or exogenous) for iron reduction at a distance[48]. Likewise, the cultivation medium may include variable amounts of inorganic salts and organic matter, which might be bound to the surface of iron oxides[49].

Finally, microorganisms could also act as a substitute for heat treatment. The idea would be to use iron-oxidizing microorganisms to bio-transform magnetite into ferric iron oxides such as siderite, hematite, or maghemite[50,51,52]. This innovative combination could further decrease energy consumption as it could eliminate the heat treatment step which involves temperatures around 1173 K. Validation of the concept of bio-mining of Martian regolith to produce bio-magnetite, magnetic precipitation, and bio-oxidation (as a substitute for heat treatment) followed by alkaline electrolysis for iron production will be the subject of further studies.

Conclusion

In this work, ferrimagnetic bio-magnetite was bio-mineralized from a superparamagnetic iron oxide/hydroxide using the iron-reducing bacterium *Carboxydothermus ferrireducens*. The obtained material showed full magnetic properties and raised the prospect of magnetic precipitation of iron-bearing phases from low-grade iron resources. The resulting bio-magnetite also opens up the possibility of depositing iron at 90 °C using alkaline electrolysis. Indeed, a successful electrochemical conversion of 25(1) wt.% to Fe(0) with a current efficiency of 9(2) % was achieved after 20 h electrolysis of bio-magnetite.

Intermediate heat treatment of the bio-magnetite led to a complete oxidation to bio-hematite, which thermodynamically requires less decomposition energy for electrolysis. Indeed, the reduction iron yield was improved to 67(1) % and the current efficiency to 63(3) %. The estimated energy consumption of the power required for electrolysis and heat treatment steps is around 17.9 MJ/kg, which is competitive with the current industrial processes.

We also highlighted the role of microstructure on reducibility. It was shown that particle agglomeration during heat treatment reduces the total surface area and the number of active sites available for undesirable side reactions such as hydrogen evolution. The treatment also improves the crystallinity of the materials, facilitating uniform electron flow, which is essential for electrochemical stability during reduction. As a result, the heat-treated materials exhibit improved electrochemical reduction rates and efficiencies. In this way, a greater proportion of the electrical energy is effectively used for the desired reduction reactions, rather than being lost to side reactions. However, controlled heat treatment is key, as too much agglomeration could hinder the diffusion of electrolytes into the pellet, the release of oxygen ions, and the propagation of reduction[53].

The findings of this research allowed us to propose a forward-looking concept for utilizing low-grade iron resources such as sediments and also the extraterrestrial Martian soil for iron production. The introduced approach could lead to more sustainable mining practices and bridge the gap between current needs for resource efficiency and future demands in both terrestrial and extraterrestrial environments. The combination of biological, thermal, and electrochemical processes to refine ores is innovative and could lead to the development of new types of metal extraction and processing technologies.

Materials and methods

Bio-mineralization

The iron oxide/hydroxide was prepared by gradually adding NaOH 10 M in a solution of $FeCl_3 \cdot H_2O$ (108 g/L) until the pH was stabilized at 7. The iron oxide/hydroxide suspension was then centrifuged and washed with deionized water.

Bio-magnetite was prepared by providing this iron oxide/hydroxide to *Carboxydothermus ferrireducens*, an iron-reducing bacterium, as the terminal electron acceptor for anaerobic respiration. C. ferrireducens was purchased from DSMZ (DSM 11255). It is a thermophile (323 to 347 K) and a facultative autotroph, isolated from hot springs in Yellowstone National Park, Wyoming, USA. To simplify cultivation, the bacterium was cultivated organoheterotrophically with glycerol as the carbon and energy source. It was cultivated anaerobically in 1 L Schott bottles.

The medium contained, per liter of deionized water: 0.33 g of KH_2PO_4, 0.33 g of NH_4Cl, 0.33 g of KCl, 0.33 g of $MgCl_2 \cdot 6H_2O$, 0.33 g of $CaCl_2 \cdot 2H_2O$, 0.2 g of $MgSO_4 \cdot 7H_2O$, 2.5 g of $NaHCO_3$, 0.1 g of yeast extract, and 1 mL of Wolfe's mineral elixir (trace elements solution, DSMZ). All chemicals were > 99 % pure and purchased from Carl Roth (Germany), Merck (Germany), or VWR International (United States). The medium was prepared in an anaerobic chamber, adjusted to pH 6.8 with 1 M HCl, and autoclaved. $CaCl_2 \cdot 2H_2O$ was added to the medium after autoclaving, from an autoclaved concentrated solution. The trace elements

solution contained, per liter of deionized water: 30 g of $MgSO_4 \cdot 7H_2O$, 5 g of $MnSO_4 \cdot nH_2O$, 10 g of NaCl, 1 g of $FeSO_4 \cdot 7H_2O$, 1.8 g of $CoCl_2 \cdot 6\ H_2O$, 1 g of $CaCl_2 \cdot 2H_2O$, 1.8 g of $ZnSO_4 \cdot 7H_2O$, 0.1 g of $CuSO_4 \cdot 5H_2O$, 0.18 g of $AlK(SO_4)_2 \cdot 12H_2O$, 0.1 g of H_3BO_3, 0.1 g of $Na_2MoO_4 \cdot 2H_2O$, 2.8 g of $(NH_4)_2Ni(SO_4)_2 \cdot 6\ H_2O$, 0.1 g of $Na_2WO_4.2H_2O$, and 0.1 g of Na_2SeO_4. The salts were dissolved after adjusting the pH to 1.0 with sulfuric acid. The medium was distributed to three 1 L cultivation bottles containing each 500 mL of medium. After autoclaving, the cultivation bottles were complemented with glycerol (40 mM), iron oxide/hydroxide (100 mM of Fe^{3+}), and $Na_2S \cdot 9H_2O$ (0.05 mM of Na_2S) from concentrated solutions. The glycerol-concentrated solution was autoclaved while the $Na_2S \cdot 9H_2O$ solution was filter-sterilized. The iron oxide/hydroxide was not autoclaved to prevent crystallization. The cultivation bottles were inoculated with 8 mL of iron oxide/hydroxide-reducing *Carboxydothermus* cultures, and placed in an incubator (Heratherm, Thermo Fisher Scientific, USA) at 338 K and magnetically stirred at 400 rpm for about 48 h until the particles in the medium had become black and magnetic. The concentration of Fe^{2+} was measured spectrophotometrically with the ferrozine assay [54]. Before measurements, 1 mL of the sample was mixed with 1 mL of 4 M HCl until the particles were visually dissolved (less than an hour to a few days for the final samples with black magnetic particles). Cells were observed during cultivation with a fluorescence microscope. Liquid samples were stained with 2 µg/mL of 4′,6-diamidine-2-phenylindole (DAPI) (Carl Roth, Germany), illuminated with ultraviolet light (385 nm), and observed with a Zeiss Microscope Axioscope 7 (Carl Zeiss, Germany) at 500x magnification (reflected light at 465 nm). At the end of the cultivation, the magnetic particles were rinsed with deionized water once and dried at room temperature. In total, about 14 g of black, magnetic particles were obtained from the 3 cultures.

Sample Preparation

The heat treatment was done under air at 1173 K for 3 h. The commercial materials used were hematite powder (Carl Roth, ≥ 95 %, 400 mesh) and magnetite powder (Thermo Scientific, ≥ 97 %, 325 mesh). An electrolyte solution was prepared by dissolving 10 M NaOH (VWR, 99.3 %) in water. The electrolyte solution, being highly concentrated, was aimed at minimizing the hydrogen evolution reaction (HER) and reducing water loss.[55] A Martian regolith simulant, MGS-1 (Space Resource Technologies (SRT), batch code: 002-05-001-0621, mean particle size: 90 μm) was analyzed to understand the mineral composition. The cathode pellet formation was innovatively performed using a conductive Ag-paste (MG Chemicals, product code: 8330S-A) to inhibit any mineral phase alteration of precursors during the typical pressing-sintering pelletization. Approximately 1 g of powder was used to produce each disk-shaped pellet (diameter: 10 mm, thickness: 3 mm). Around 2 mL of the glue was used for each pellet, which was then cured at 353 K for 2 h.

To account for the potential effect of silver epoxy on the electrochemical measurements, electrolysis was performed using samples containing only the Ag paste. Initially, it was confirmed that silver was not involved in the electrochemical reaction, as no phase change was observed post-electrolysis (confirmed by XRPD analysis). The charge resulting from this control experiment was measured (2420 C for 20 h) and subsequently subtracted from the total electrical charge obtained from the main electrolysis experiments. This ensured that the HER associated with the silver was excluded from the calculations.

Electrochemical experiments

Electrical contacts were established by connecting a Kanthal® wire to a hole in the center of the cathode pellet. An anion exchange membrane (Reichelt Chemietechnik, MA-3475) was employed to separate the electrodes. Before each test, the membrane was activated by immersing it in a 10 % salt solution at 328 K for 3 h. The electrochemical tests were conducted in a Teflon H-cell separated by an anion exchange membrane (AEM). The working electrode consisted of either iron oxide/hydroxide, bio-magnetite, bio-hematite, commercial magnetite,

or commercial hematite pellets connected to the wire. A reference electrode of Ag|AgCl|KCl (3.5 M) with a potential of +0.205 V vs. the standard hydrogen electrode (Xylem Analytics) was utilized. Based on insights from our prior study[5], we employed Ni/Fe as a non-contaminating inert counter electrode, which also catalyzes the oxygen evolution and reduces the anodic overpotential[56]. This anode electrode was a rod-shaped Ni36/Fe64 alloy, with a diameter of 20 mm and a height of 100 mm. The measurement equipment employed was a potentiostat (IPS Elektroniklabor, PGU-1A-OEM). Before conducting electrochemical tests, the cathode electrodes were immersed in the electrolyte (10 M NaOH with a pH of 15) for 30 minutes to ensure proper wetting.

To screen electrochemical redox peaks at the hematite/electrolyte interface, cyclovoltammetry (CV) tests were performed. The CVs were recorded with a scan rate of 50 mV/s, within a range of 1.8 V to +0.5 V relative to the open circuit potential, and repeated for 3 cycles.

Electrolysis tests (chronoamperometry) were conducted by applying a constant potential of -1.4 V vs. the Ag/AgCl reference electrode for 20 or 5 h while measuring the corresponding current. A second potentiostat (IPS Elektroniklabor, IMP 83 PC T-BC) was employed to measure the total cell voltage during electrolysis for the sake of energy calculations. All electrochemical tests were conducted under an argon-protected atmosphere to suppress the carbon parasitic reaction loop.[5]

Sample characterization

After the reduction process, the electrodes were pulled above the electrolyte line and dried under argon to be pulled out after the cell was cooled. To eliminate any residual electrolyte, the cathode samples were subjected to Soxhlet extraction using water as the solvent for a duration of up to 5 h.[57] Subsequently, the samples were dried in an oven at 80 °C for 1 h and weighed. To characterize the samples, they were ground and subjected to X-ray powder diffraction (XRPD) analysis.[58] XRPD measurements were carried out on a Bruker D8 Discover diffractometer using CuKα1,2 radiation ($\lambda_{K\alpha1}$ = 154.05929(5) pm, $\lambda_{K\alpha2}$ = 154.4414(2) pm) in Bragg-Brentano geometry. Data was collected at ambient conditions in a range of 20° to 100° 2θ, with a step width of 0.0149° 2θ and a measurement time of 0.3 seconds per step using an energy-discriminating LynxEye-XET multi-strip detector. The Rietveld refinements were performed using TOPAS V6.0 (Bruker AXS). The average crystallite size of the amorphous scattering samples was determined using the EnvACS approach.[32] For elemental mapping of selected sponges produced, SEM (JEOL, JMS-6510 model) and EDX (Bruker, XFlash 410-M model) analyses were performed. The specific surface area of the sample was measured using a Brunauer-Emmett-Teller (BET) surface area analyzer, Belsorb Mini (Microtrac), with N_2 as an adsorption gas. Samples were pre-treated at 393 K for 3 h in a vacuum.

References

1. Oarga-Mulec, A., Luin, U. & Valant, M. Back to the future with emerging iron technologies. *RSC Adv.* 20765–20779 (2024) doi:10.1039/d4ra03565h.
2. Kim, J. *et al.* Decarbonizing the iron and steel industry: A systematic review of sociotechnical systems, technological innovations, and policy options. *Energy Res. Soc. Sci.* **89**, 102565 (2022).
3. Wang, X. *et al.* Research progress in the preparation of iron by electrochemical reduction route without CO2 emissions. *J. Appl. Electrochem.* **53**, 1521–1536 (2023).
4. Ranzani, A. *et al.* Modelling a new , low CO2 emissions , hydrogen steelmaking process To cite this version : HAL Id : hal-00943356 Modelling a new , low CO 2 emissions ,. (2014).
5. Fayaz, R. *et al.* Deoxidation Electrolysis of Hematite in Alkaline Solution: Impact of Cell Configuration and Process Parameters on Reduction Efficiency. *ChemElectroChem* **10**, 1–9 (2023).

6. Jovičević-Klug, M., Souza Filho, I. R., Springer, H., Adam, C. & Raabe, D. Green steel from red mud through climate-neutral hydrogen plasma reduction. *Nature* **625**, 703–709 (2024).
7. Wang, R. R., Zhao, Y. Q., Babich, A., Senk, D. & Fan, X. Y. Hydrogen direct reduction (H-DR) in steel industry—An overview of challenges and opportunities. *J. Clean. Prod.* **329**, 129797 (2021).
8. Childs, C. W. Ferrihydrite: A review of structure, properties and occurrence in relation to soils. *Soil Conserv.* (1992).
9. Filip, J. *et al.* Environmental applications of chemically pure natural ferrihydrite. *Environ. Sci. Technol.* **41**, 4367–4374 (2007).
10. Bazylinski, D. A., Frankel, R. B. & Konhauser, K. O. Modes of biomineralization of magnetite by microbes. *Geomicrobiol. J.* **24**, 465–475 (2007).
11. Hecht, M. *et al.* Mars Oxygen ISRU Experiment (MOXIE). *Space Sci. Rev.* **217**, (2021).
12. Gayen, P., Sankarasubramanian, S. & Ramani, V. K. Fuel and oxygen harvesting from Martian regolithic brine. *Proc. Natl. Acad. Sci.* **117**, 31685–31689 (2020).
13. Hinterman, E. Simulating oxygen production on Mars for the Mars Oxygen In-Situ Resource Utilization Experiment. *Acta Astronaut.* **170**, 678–685 (2020).
14. Schlüter, L. & Cowley, A. Review of techniques for In-Situ oxygen extraction on the moon. *Planet. Space Sci.* **181**, 104753 (2020).
15. Ehlmann, B. L. & Edwards, C. S. Mineralogy of the Martian surface. *Annu. Rev. Earth Planet. Sci.* **42**, 291–315 (2014).
16. Cannon, K. M., Britt, D. T., Smith, T. M., Fritsche, R. F. & Batcheldor, D. Mars global simulant MGS-1: A Rocknest-based open standard for basaltic martian regolith simulants. *Icarus* **317**, 470–478 (2019).
17. Schwandt, C., Hamilton, J. A., Fray, D. J. & Crawford, I. A. The production of oxygen and metal from lunar regolith. *Planet. Space Sci.* **74**, 49–56 (2012).
18. Humbert, M. S., Brooks, G. A., Duffy, A. R., Hargrave, C. & Rhamdhani, M. A. Thermophysical property evolution during molten regolith electrolysis. *Planet. Space Sci.* **219**, 105527 (2022).
19. Schreiner, S. S., Sibille, L., Dominguez, J. A. & Hoffman, J. A. A parametric sizing model for Molten Regolith Electrolysis reactors to produce oxygen on the Moon. *Adv. Sp. Res.* **57**, 1585–1603 (2016).
20. Mohandas, K. S. Direct electrochemical conversion of metal oxides to metal by molten salt electrolysis: A review. *Trans. Institutions Min. Metall. Sect. C Miner. Process. Extr. Metall.* **122**, 195–212 (2013).
21. Chen, G. Z. the Ffc Cambridge Process for Metal Production: Principle, Practice and Prospect. *3rd Int. Slag Valoris. Symp.* 217–233 (2013).
22. Lomax, B. A. *et al.* Proving the viability of an electrochemical process for the simultaneous extraction of oxygen and production of metal alloys from lunar regolith. *Planet. Space Sci.* **180**, 104748 (2020).
23. Meurisse, A. *et al.* Lower temperature electrochemical reduction of lunar regolith simulants in molten salts. *Planet. Space Sci.* **211**, (2022).
24. Gumulya, Y., Zea, L. & Kaksonen, A. H. In situ resource utilisation: The potential for space biomining. *Miner. Eng.* **176**, 107288 (2022).
25. Cockell, C. S. *et al.* Space station biomining experiment demonstrates rare earth element extraction in microgravity and Mars gravity. *Nat. Commun.* **11**, 1–11 (2020).
26. Castelein, S. M. *et al.* Iron can be microbially extracted from Lunar and Martian regolith simulants and 3D printed into tough structural materials. *PLoS One* **16**, 1–21 (2021).
27. Volger, R. *et al.* Mining moon & mars with microbes: Biological approaches to extract

iron from Lunar and Martian regolith. *Planet. Space Sci.* **184**, 104850 (2020).
28. Bösing, I., La Mantia, F. & Thöming, J. Modeling of electrochemical oxide film growth-a PDM refinement. *Electrochim. Acta* **406**, (2022).
29. Hansford, G. S. & Vargas, T. Chemical and electrochemical basis of bioleaching processes. *Process Metall.* **9**, 13–26 (1999).
30. Gavrilov, S. N. *et al.* Novel Extracellular Electron Transfer Channels in a Gram-Positive Thermophilic Bacterium. *Front. Microbiol.* **11**, 1–21 (2021).
31. Slobodkin, A., Reysenbach, A. L., Strutz, N., Dreier, M. & Wiegel, J. Thermoterrabacterium ferrireducens gen. nov., sp. nov., a thermophilic anaerobic dissimilatory Fe(III)-reducing bacterium from a continental hot spring. *Int. J. Syst. Bacteriol.* **47**, 541–547 (1997).
32. Gesing, T. M. & Robben, L. Determination of the average crystallite size and the crystallite size distribution: The envelope function approach EnvACS. *J. Appl. Crystallogr.* (2024) doi:10.1107/S1600576724007362.
33. Beveridge, T. J. & Murray, R. G. E. Sites of metal deposition in the cell wall of Bacillus subtilis. *J. Bacteriol.* **141**, 876–887 (1980).
34. Fein, J. B. Quantifying the effects of bacteria on adsorption reactions in water-rock systems. *Chem. Geol.* **169**, 265–280 (2000).
35. Sk, M. M., Pradhan, P., Patra, B. K. & Guria, A. K. Green biomass derived porous carbon materials for electrical double-layer capacitors (EDLCs). *Mater. Today Chem.* **30**, (2023).
36. Green, D. W. & Perry, R. H. *Perry's Chemical Engineers' Handbook*. (McGraw-Hill, 2008).
37. Heidari, A., Niknahad, N., Iljana, M. & Fabritius, T. A review on the kinetics of iron ore reduction by hydrogen. *Materials (Basel).* **14**, (2021).
38. Spreitzer, D. & Schenk, J. Reduction of Iron Oxides with Hydrogen—A Review. *Steel Res. Int.* **90**, (2019).
39. Zhang, L., Wu, H. Bin & Lou, X. W. Iron-oxide-based advanced anode materials for lithium-ion batteries. *Adv. Energy Mater.* **4**, 1–11 (2014).
40. Pervez, S. A. *et al.* Comparative electrochemical analysis of crystalline and amorphous anodized iron oxide nanotube layers as negative electrode for LIB. *ACS Appl. Mater. Interfaces* **6**, 11219–11224 (2014).
41. Sohn, H. Y. & Mohassab, Y. *Greenhouse Gas Emissions and Energy Consumption of Ironmaking Processes*. *Springer, Cham* (2016). doi:https://doi.org/10.1007/978-3-319-39529-6_25.
42. Perez-Gonzalez, T. *et al.* Magnetite biomineralization induced by Shewanella oneidensis. *Geochim. Cosmochim. Acta* **74**, 967–979 (2010).
43. Zachara, J. M., Kukkadapu, R. K., Fredrickson, J. K., Gorby, Y. A. & Smith, S. C. Biomineralization of poorly crystalline Fe(III) oxides by dissimilatory metal reducing bacteria (DMRB). *Geomicrobiol. J.* **19**, 179–207 (2002).
44. Dong, H. *et al.* Mineral transformation associated with the microbial reduction of magnetite. *Chem. Geol.* **169**, 299–318 (2000).
45. Slobodkin, A. I. Thermophilic microbial metal reduction. *Mikrobiologiya* **74**, 581–595 (2005).
46. Piepenbrock, A., Dippon, U., Porsch, K., Appel, E. & Kappler, A. Dependence of microbial magnetite formation on humic substance and ferrihydrite concentrations. *Geochim. Cosmochim. Acta* **75**, 6844–6858 (2011).
47. Kong, P., Ebihara, M. & Palme, H. Siderophile elements in Martian meteorites and implications for core formation in Mars. *Geochim. Cosmochim. Acta* **63**, 1865–1875 (1999).
48. Nevin, K. P. & Lovley, D. R. Mechanisms for Fe(III) oxide reduction in sedimentary

environments. *Geomicrobiol. J.* **19**, 141–159 (2002).
49. Cornell, R. M. & Schwertmann, U. *Adsorption of Ions and Molecules*. *The Iron Oxides* (2003). doi:10.1002/3527602097.ch11.
50. Weber, K. A., Achenbach, L. A. & Coates, J. D. Microorganisms pumping iron: Anaerobic microbial iron oxidation and reduction. *Nat. Rev. Microbiol.* **4**, 752–764 (2006).
51. Brown A.*, D., Sherrif L., B. & Sawicki A., J. Microbial transformation of magnetite to hematite. *Geochim. Cosmochim. Acta* **61**, 3341–3348 (1997).
52. Ohenhen, L. O. *et al.* Microbially Induced Anaerobic Oxidation of Magnetite to Maghemite in a Hydrocarbon-Contaminated Aquifer. *J. Geophys. Res. Biogeosciences* **127**, 1–24 (2022).
53. Chen, G. Z., Gordo, E. & Fray, D. J. Direct electrolytic preparation of chromium powder. *Metall. Mater. Trans. B Process Metall. Mater. Process. Sci.* **35**, 223–233 (2004).
54. Viollier, E., Inglett, P. W., Hunter, K., Roychoudhury, A. N. & Cappellen, P. Van. The Ferrozine method revisted. *Appl. Geochemistry* **15**, 785–790 (2000).
55. Wang, S. lan, Haarberg, G. M. & Kvalheim, E. Electrochemical Behavior of Dissolved Fe2O3 in Molten CaCl2-KF. *J. Iron Steel Res. Int.* **15**, 48–51 (2008).
56. Trotochaud, L., Young, S. L., Ranney, J. K. & Boettcher, S. W. Nickel-Iron oxyhydroxide oxygen-evolution electrocatalysts: The role of intentional and incidental iron incorporation. *J. Am. Chem. Soc.* **136**, 6744–6753 (2014).
57. Hyslop, D. J. S., Abdelkader, A. M., Cox, A. & Fray, D. J. Utilization of Constant Current Chronopotentiometry to Synthesize a Co–Cr Alloy. *J. Electrochem. Soc.* **157**, E111 (2010).
58. Qiao, J., Liu, Y., Hong, F. & Zhang, J. A review of catalysts for the electroreduction of carbon dioxide to produce low-carbon fuels. *Chem. Soc. Rev.* **43**, 631–675 (2014).